Optical switching at 1.55 μm in silicon microring resonators using phase change materials

Miquel Rudé,[1, a)] Josselin Pello,[2] Robert E. Simpson,[3] Johann Osmond,[1] Gunther Roelkens,[4] Jos J.G.M. van der Tol,[2] and Valerio Pruneri[1, 5]

[1)] *ICFO-Institut de Ciències Fotòniques, 08860 Castelldefels, Spain*
[2)] *Eindhoven University of Technology, 5600 MB Eindhoven, Netherlands*
[3)] *Singapore University of Technology and Design, 138683 Singapore, Singapore*
[4)] *Ghent University - IMEC, 9000 Ghent, Belgium*
[5)] *ICREA-Institució Catalana de Recerca i Estudis Avançats*

(Dated: 16 May 2013)

A novel optical switch operating at a wavelength of 1.55 μm and showing a 12 dB modulation depth is introduced. The device is implemented in a silicon microring resonator using an overcladding layer of the phase change data storage material $Ge_2Sb_2Te_5$ (GST), which exhibits high contrast in its optical properties upon transitions between its crystalline and amorphous structural phases. These transitions are triggered using a pulsed laser diode at $\lambda = 975$ nm and used to tune the resonant frequency of the microring resonator and the resultant modulation depth of the 1.55 μm transmitted light.

The ever-increasing demand for high speed optical communication networks is driving the development of new photonic devices that can process optical signals in a reliable, low-cost manner. Among competing technologies, Si-based devices have emerged as one of the main candidates for such applications, and several devices, including modulators[1–5], add-drop filters[6] and wavelength division multiplexers (WDM)[7] have already been demonstrated. An important branch of this technology is the ability to program reconfigurable optical circuits. Indeed, a reprogrammable optical circuit that can hold its configuration without an external continuous source is extremely desirable for a multitude of applications ranging from photonic routers to optical cognitive networks. Recently, new solutions for non-volatile photonic memories have been proposed, involving the use of phase-change materials (PCM) and microring resonators[8,9].

Herein, a non-volatile Si microring resonator optical switch is demonstrated. A thin film of the phase-change material[10](PCM) $Ge_2Sb_2Te_5$(GST), which is commonly encountered in optical and electrical data storage applications[11–14], is used to switch the resonant frequency and Q-factor of the microring resonator. GST shows high optical contrast between its amorphous, covalently bonded, and crystalline, resonantly bonded, structural phases[15–18]($n_{cryst} - n_{amorph} = 2.5$; $k_{cryst} - k_{amorph} = 1$ at 1.55 μm)[19]. Moreover, transitions between the two phases can take place on a sub-ns timescale[20,22] while the resulting final state is stable for several years. These characteristics deem this material appropriate for application in reconfigurable optical circuits.

The device, shown in Fig. 1, consists of a Si microring resonator with a bend radius of 5 μm and a coupling region of 3 μm, on top of which a GST thin film with an area of 3×1.5 μm^2 has been deposited. A second Si microring with identical dimensions but free of GST is used as a reference during the measurements. A 200 nm gap separates both microrings from a Si strip waveguide (220×440 nm^2) with grating couplers[23] at both ends, which are used to deliver light into the device and monitor the transmitted spectrum using single-mode fibers (SMF).

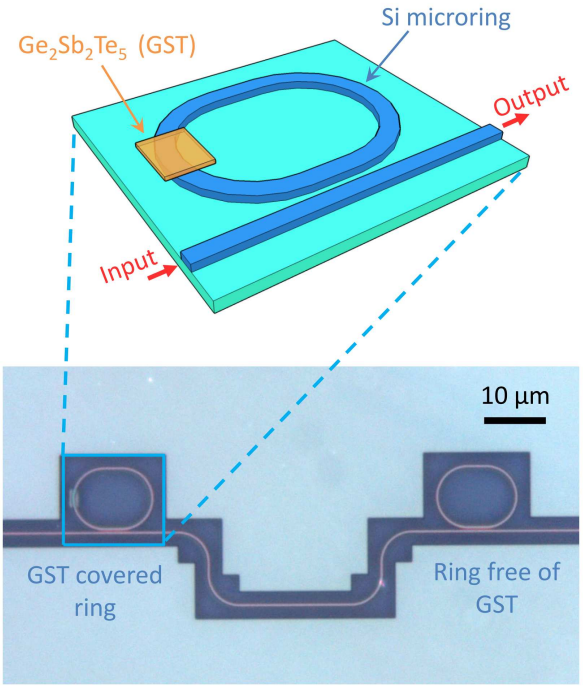

FIG. 1. Optical microscope image showing the two microrings coupled to a waveguide. The first of them (left) contains the overcladding layer of GST.

The microrings, waveguides and grating couplers were

[a)] miquel.rude@icfo.es

fabricated on top of a silicon-on-insulator (SOI) substrate with 2 μm of buried oxide using 248 nm deep UV lithography, following a previously developed method[24]. In order to control the overlap of the mode propagating inside the microring with the GST, a thin buffer layer (50 nm) of SiO_2 was deposited on top of the Si waveguide using plasma-enhanced chemical vapor deposition (PECVD). Subsequently, polymethylmethracylate resist (PMMA) was spun on the SOI die and the area where the GST was to be deposited was opened using e-beam lithography. A 20 nm thick GST film was deposited into this area using radio frequency (RF) sputtering from two stoichiometric targets of GeTe and Sb_2Te_3. X-ray diffraction from other GST films, which were prepared under the same conditions, confirmed the structural phase of the film to be amorphous. To avoid oxidation of this layer and achieve good thermal isolation a 20 nm film of Si_3N_4 was grown on top of the GST by reactive DC sputtering Si using a mixture of Ar and N_2 as the process gases. The sputtering conditions for these films are summarized in Table I. The sample was then put in an acetone bath for 30 minutes to remove the PMMA and lift off the excess material. Finally the device was rinsed with isopropanol and blow dried.

TABLE I. Sputtering conditions for the $Ge_2Sb_2Te_5$ and Si_3N_4 films. The targets in all cases are 3" in diameter.

	$Ge_2Sb_2Te_5$		Si_3N_4	
Targets	GeTe	Sb_2Te_3	Si	
Power (type)	50 W (RF)	45 W (RF)	40 W (DC)	
Process gases	Ar		Ar	N_2
Gas flow	10 sccm		7 sccm	3 sccm
Gas pressure	3.75 mTorr		3.75 mTorr	
Time	90 s		1200 s	
Temperature	298 K		298 K	

Measurements were performed using the optical set-up shown in Fig. 2. Phase transitions in the GST layer were triggered by heating a 1 μm spot with focused laser radiation at $\lambda = 975$ nm. The electrical current driving the laser was maintained at a sub-threshold level during the experiment. Electrical pulses with tunable length and amplitude were generated in a function generator (Agilent 33220A, 20 MHz) and amplified by a high-gain amplifier (MiniCircuits LZY-22+, 43 dB gain) before being sent to the laser through a bias-T circuit. The output optical pulses were coupled into a SMF, collimated and focused down to a diameter of 1 μm on the sample using a 0.6 NA (50x) objective. Homogeneous illumination of the sample was achieved using a white LED and an aspheric condenser lens and cross-polarizers were used to optimize the contrast of the image. An additional short-pass infrared filter ($\lambda_{cutoff} = 950$ nm) was added to attenuate the laser beam and avoid damage to the camera. Precise alignment of the laser spot with the GST was achieved by monitoring the reflected laser spot and the sample image with a CCD camera and then using a 3-axis stepper motorized stage to control the sample position and the focus of the 975 nm laser radiation.

Two SMF were used to couple light from a broadband ($\lambda_{min} = 1520$ nm to $\lambda_{max} = 1580$ nm) amplified spontaneous emission (ASE) source. The transmitted spectrum was recorded with an optical spectrum analyzer (OSA). Both fibers were cleaved and mounted on holders to ensure 10° incidence with the sample. Optimal coupling to and from the waveguide was achieved using two 3-axis micro-positioners. The device temperature was controlled by placing the sample on top of a thermo electrical cooler (TEC).

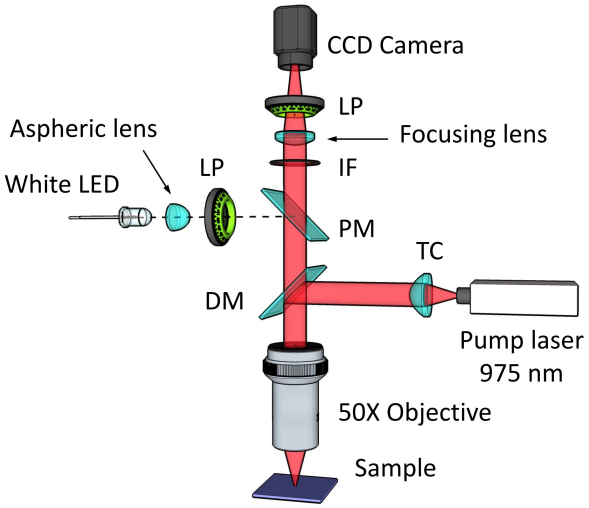

FIG. 2. Schematic of the experimental set-up (LP: Linear polarizer, DM: Dichroic mirror, IF: Infrared filter, PM: Pellicle mirror, TC: Triplet collimator).

The laser pulse time and power for crystallization and re-amorphization of the GST film are strongly dependent on the composition, thickness and the thermal properties of surrounding materials[25,26]. In order to confirm switching, a planar test sample with the same structure as that found on top of the microring was fabricated on a SOI substrate. The switching parameters for this sample were then optimized by iteratively increasing the laser pulse time and power. Crystallized marks, which appear as brighter areas in the reflected image due to their higher refractive index, were repeatedly created with a laser power of 12 mW and a pulse duration of 300 ns (FWHM, 80 ns edge), while reamorphization of a crystallized area was achieved with laser pulses of 45 mW and a duration of 20 ns (FWHM, 8 ns edge). The diameter of these spots was approximately the same as the laser beam, i.e. 1 μm.

A final important step before proceeding with the measurements was to analyze the effect of temperature on the transmission spectrum. Si microrings are sensitive to external variations in temperature, mainly due to the thermo-optic effect in Si[27,28]. An increase of just 1 °C

(which increases n_{eff} proportionally) can manifest as a non negligible red-shift in the resonant wavelength. By scanning the temperature from 20° to 30° with the TEC we found a value for this shift of $d\lambda/dT = 71$ pmK^{-1}, in agreement with previous studies on similar devices[29,30]. As will be seen later, this shift is comparable to the increase in λ_{res} upon crystallization of the GST film. Therefore, the temperature during the experiment was fixed at 22 ± 0.02 °C.

Fig. 3 shows the full transmission spectrum of the device shown in Fig. 1 with the GST set in its amorphous phase. Since the device contains two microrings in series, the dips in the figure appear grouped in pairs. The left one in each pair corresponds to the microring with GST and is modified upon phase transitions, while the right one, corresponding to the bare microring, is used as a reference.

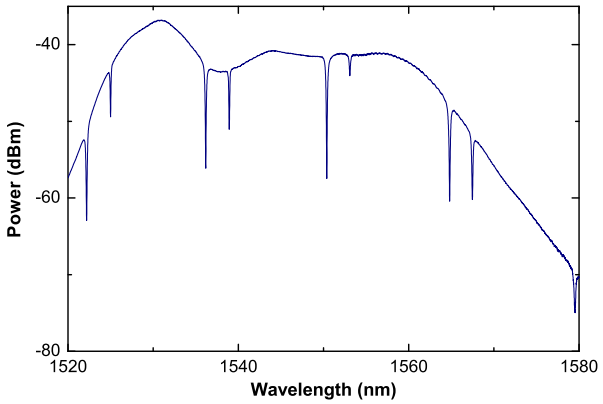

FIG. 3. Transmission spectrum between 1520 and 1580 nm. Note that the envelope of the spectrum is not flat due to ASE source.

Starting from this initial state, crystallization pulses with the parameters found above were used to crystallize the GST film. Due to the GST area (3x1.5 μm^2) being larger than the focused laser spot (1 μm) it was necessary to move (1 μm steps) the laser across the area and repeatedly apply the crystallization pulse until the complete area of GST was crystallized. In actuality this could be achieved with just 3 shots along the axis waveguide (Fig. 4(a)). The same process was repeated using reamorphization pulses to recover the transmissivity at λ=1.55 μm, thus completing a full cycle (Fig. 4(b)).

The effect of the structural phase transitions on the device transmission was analyzed using the power transfer function of a microring, which is given by[31]

$$\frac{P_{out}}{P_{in}} = \frac{\tau^2 - 2t\tau\cos\phi + t^2}{1 - 2t\tau\cos\phi + t^2\tau^2} \qquad (1)$$

Here τ is the decay constant of the optical mode inside the microring, which determines the losses $\alpha = -2\log\tau/L$, t is the electric field transmission coefficient

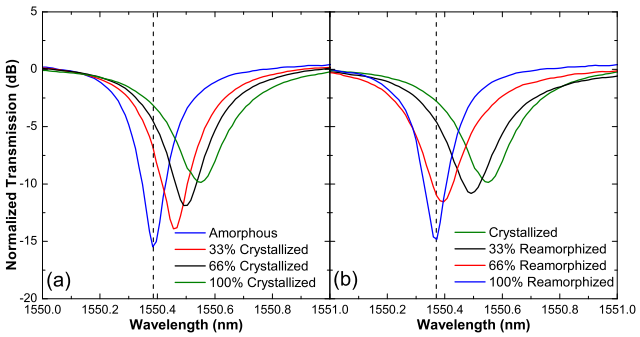

FIG. 4. Evolution of the spectrum during crystallization (a) and reamorphization (b) of the 1.5x3 μm GST area.

at the coupler and $\phi = \frac{2\pi}{\lambda} L n_{eff}$, is the phase shift after one round trip. By fitting the data in Fig. 4 to (1) it was possible to determine the evolution of these values during one crystallization/reamorphization cycle (see Table II).

TABLE II. Evolution of the microring parameters during the cycle.

State	λ_{res}(nm)	n_{eff}	τ	t	Q	α(cm^{-1})
Amorphous	1550.384	2.3204	0.986	0.983	5656	7.570
33% Cryst.	1550.456	2.3205	0.977	0.983	4433	12.326
66% Cryst.	1550.492	2.3206	0.974	0.983	4115	13.983
Crystallized	1550.552	2.3207	0.968	0.983	3641	16.841
33% Ream.	1550.492	2.3206	0.972	0.983	3922	15.145
66% Ream.	1550.396	2.3205	0.974	0.983	4051	14.454
Reamorphized	1550.372	2.3204	0.986	0.983	5411	7.160

One can see that the optical properties of the final amorphous state are quite similar to that of the inital one, with maximum differences in the values lying around 5% , indicating that the switch performance is robust and reversible. If one considers the out-of-equilibrium nature of the sputter deposition process, then small differences between the optical properties of the as-deposited amorphous state and the laser reamorphized state are to be expected. Indeed it is normally necessary to cycle GST data storage devices more than 100 times before the electrical properties of the amorphous state converge to a stable value[14]. Table II also shows a clear effect of the amorphous to crystalline phase transition on the transmission. The increase in the refractive index of GST upon crystallization increases the averaged out effective refractive index of the ring by 0.0003, producing a red shift of $\lambda_{cryst} - \lambda_{amorph} = 168$ pm, while the higher absorption coefficient increases the losses α in the microring (thus decreasing τ and the Q factor). As expected, the transmission coefficient t, which only depends on the coupling efficiency between the waveguide and the microring, remains the same in all cases. Finally, labelling the amorphous phase as the 'off' state and the crystalline one as the 'on' state, the combination of both effects pro-

duces a modulation of 12.36 dB at $\lambda = 1550.384$ nm. In this case, the insertion loss in the 'on' state is -2.5 dB.

All of the aforementioned measurements were static, but it is also interesting to investigate the time response of the device. For this purpose, the ASE source was replaced by a tunable laser (HP 8168F) and the OSA by a fast photodiode (ThorLabs PDA8GS, <1 ns rise time). In this way the laser was tuned at the respective λ_{res} of the amorphous/crystalline state and the response of the device during one crystallization/reamorphization pulse was monitored by an oscilloscope (see Fig. 5).

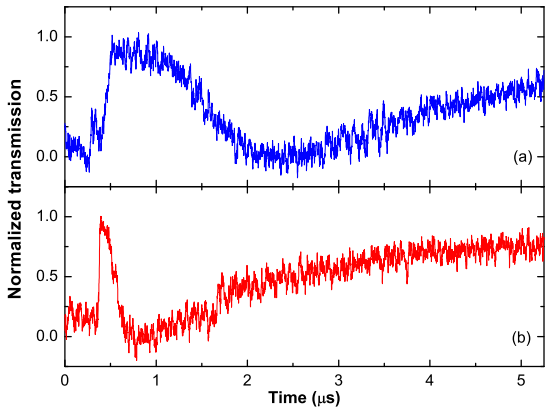

FIG. 5. Time response of the device during (a) a crystallization pulse ($\lambda_{res} = 1550.384$ nm) and (b) a reamorphization pulse ($\lambda_{res} = 1550.552$ nm). Increasing values in the graph indicate higher transmission at that wavelength.

Analysis of Fig. 5(a) and 5(b) suggests that the time response can be explained by two different effects. First, when a pulse reaches the device after 0.3 μs the GST film starts to heat up and the phase transition is initiated. During this transition the transmission in the device increases until the graph reaches its inital maximum value. At this point the phase transition is done, and application of more heat (as long as it is not high enough to damage the GST) does not change the optical properties of the film. If no other effect took place the temporal response would be just a single step. But in parallel and on a slower timescale the local heat generated by the laser also propagates to the underlying Si through the SiO_2 buffer layer, which has low thermal conductivity, and locally increases n_{eff} in the microring, hence decreasing again the transmission. Once the laser pulse ends and after some delay, the remaining heat is dissipated out of the device and the crystalline transmission level is recovered. This second process, which is much slower, dominates the temporal response of the device, which is approximately 5 μs. A similar trend can be seen when the device is reamorphized. Again the transmission is initially switched very quickly (25 ns) but the heat diffusion through the device stabilizes the system after approximately 5 μs.

In conclusion, we have demonstrated that the optical contrast of PCMs thin films can be used to reversibly tune the resonances in a Si microring between two well-defined states. Using this effect, which is triggered by means of optical pulses from an infrared laser diode, we have achieved an optical switch with an on/off ratio higher than 12 dB and response times of approximately 5 μs, operating at telecommunication wavelengths. By using heat-sinking structures with high thermal conductivity the time response of the device could be enhanced and limited only by the phase transition times of PCMs, while optimization of the microring and GST geometries could reduce the insertion loss well below 1 dB. Moreover, the ability of PCMs to be electrically switched suggests further improvements in the device, for instance, by triggering these transitions using integrated metal electrodes.

ACKNOWLEDGMENTS

This work has been funded by the Ministerio de Ciencia e Innovación through grant TEC 2010-14832.

[1] Q. F. Xu, B. Schmidt, S. Pradhan, and M. Lipson, Nature **435(7040)**, 325 (2005).
[2] G. T. Reed, G. Mashanovich, F. Y. Gardes, and D. J. Thompson, Nature Phot. **4(8)**, 518 (2010).
[3] M. Liu, X. B. Yin, E. Ulin-Avila, B. S. Jeng, T. Zentgraf, L. Ju, F. Wang, and X. Zhang, Nature **474(7349)**, 64 (2011).
[4] Q. F. Xu and M. Lipson, Opt. Express **15(3)**, 924 (2007).
[5] V. R. Almeida, C. A. Barrios, P. R. R., and M. Lipson, Nature **431**, 1081 (2004).
[6] S. Xiao, M. H. Khan, H. Shen, and M. Qi, Opt. Express **15**, 14765 (2007).
[7] Q. F. Xu, B. Schmidt, J. Shakya, and M. Lipson, Opt. Express **14(20)**, 9431 (2006).
[8] J. Pello, J. J. G. M. van der Tol, M. Rudé, R. E. Simpson, S. Keyvaninia, G. Roelkens, M. K. Smit, and V. Pruneri, in *16th European Conference on Integrated Optics and Technical Exhibition (ECIO), Barcelona, Spain* (2012).
[9] W. H. P. Pernice and H. Bhaskaran, Appl. Phys. Lett. **101**, 171101 (2012).
[10] D. Lencer, M. Salinga, B. Grabowski, T. Hickel, J. Neugebauer, and M. Wuttig, Nature Mater. **7**, 972 (2008).
[11] M. Wuttig and N. Yamada, Nature Mater. **6**, 824 (2007).
[12] A. V. Kolobov, P. Fons, A. I. Frenkel, A. L. Ankudinov, J. Tominaga, and T. Uruga, Nature Mater. **3**, 703 (2004).
[13] M. H. R. Lankhorst, B. W. Ketelaars, and R. A. M. Wolters, Nature Mater. **4**, 347 (2005).
[14] R. E. Simpson, P. Fons, A. V. Kolobov, T. Fukaya, M. Krbal, T. Yagi, and J. Tominaga, Nature Nanotech. **6**, 501 (2011).
[15] K. Shportko, S. Kremers, M. Woda, D. Lencer, J. Robertson, and M. Wuttig, Nature Mater. **7**, 653 (2008).
[16] B. Huang and J. Robertson, Phys. Rev. B **81(8)**, 081204 (2010).
[17] W. Welnic, S. Botti, L. Reining, and M. Wuttig, Phys. Rev. Lett. **98**, 236403 (2007).
[18] J. Robertson, Thin Solid Films **515**, 7538 (2007).
[19] Various, *Phase change materials: Science and applications*, edited by M. Wuttig and S. Raoux (Springer Verlag, New York, 2008).
[20] J. Hegedüs and S. R. Elliott, Nature Mater. **7**, 399 (2008).
[21] T. Matsunaga and N. Yamada, Jpn. J. Appl. Phys. **41(3B)**, 1674 (2002).
[22] D. Loke, T. H. Lee, W. J. Wang, L. P. Shi, R. Zhao, Y. C. yeo, T. C. Chong, and S. R. Elliott, Science **336(6088)**, 1556 (2012).
[23] G. Roelkens, D. Vermeulen, F. van Laere, S. Selvaraja, S. Scheer-

link, D. Taillaert, W. Bogaerts, P. Dumon, D. van Thourhout, and R. Baets, J. Nanosci. Nanotechnol. **10(3)**, 1551 (2010).
[24]P. Dumon, W. Bogaerts, V. Wiaux, J. Wouters, S. Beckx, J. Van Campenhout, D. Taillaert, B. Luyssaert, P. Bienstman, D. Van Thourhout, and R. Baets, IEEE Phot. Tech. Lett. **6(5)**, 1328 (2004).
[25]R. E. Simpson, M. Krbal, P. Fons, A. V. Kolobov, J. Tominaga, T. Uruga, and H. Tanida, Nano Lett. **10(2)**, 414 (2009).
[26]X. Wei, L. Shi, T. C. Chong, R. Zhao, and H. K. Lee, Jpn. J. Appl. Phys. **46**, 2211 (2007).
[27]F. G. Della Corte, M. Esposito Montefusco, L. Moretti, I. Rendina, and G. Cocorullo, J. Appl. Phys. **88(12)**, 7115 (2000).
[28]G. Cocorullo, F. G. Della Corte, I. Rendina, and P. M. Sarro, Sens. Actuators, A **71(1-2)**, 19 (1988).
[29]J. Teng, P. Dumon, W. Bogaerts, H. B. Zhang, X. G. Jian, X. Y. Han, M. S. Zhao, G. Morthier, and R. Baets, Opt. Express **17(17)**, 14627 (2009).
[30]W. N. Ye, J. Michel, and L. C. Kimerling, IEEE Phot. Tech. Lett. **20(11)**, 885 (2008).
[31]W. Bogaerts, P. de Heyn, T. van Vaerenbergh, K. de Vos, S. Kumar Selvaraja, T. Claes, P. Dumon, P. Bienstman, D. Van Thourhout, and R. Baets, Laser Phot. Rev. **6(1)**, 47 (2012).